Photocatalysis
https://www.sciltp.com/journals/photocatalysis

Perspective

MXenes in Photocatalysis: Emerging 2D Nanomaterials as Co-Catalysts, Heterojunction Engineering and Photothermal Enhancement

Gustavo Henrique Correia dos Santos, Hermenegildo García * and Ana Primo

Instituto de Tecnología Química CSIC-UPV, Universitat Politècnica de València-Consejo Superior de Investigaciones Científicas, Universitat Politècnica de València, Av. de los Naranjos s/n, 46022 Valencia, Spain
* Correspondence: hgarcia@itq.upv.es

How To Cite: dos Santos, G.H.C.; García, H.; Primo, A. MXenes in Photocatalysis: Emerging 2D Nanomaterials as Co-Catalysts, Heterojunction Engineering and Photothermal Enhancement. *Photocatalysis* **2026**, *2*(2), 5. https://doi.org/10.53941/photocatalysis.2026.100005

Received: 20 March 2026
Revised: 29 April 2026
Accepted: 6 May 2026
Published: 14 May 2026

Abstract: MXenes are emerging 2D nanomaterials with unique electronic, thermal, plasmonic and surface properties that make them promising components in advanced photocatalytic systems. Their high electron mobility and tunable surface chemistry enables efficient charge transport and the formation of heterojunctions with semiconductors, improving charge separation and photocatalytic performance. MXenes were initially used in photocatalysis as cocatalysts replacing noble metals in hydrogen evolution, but their high charge mobility and strong photothermal conversion opens promising opportunities for these materials form heterojunctions and in photothermal catalysis. Despite challenges related to oxidative stability, compositional and surface engineering strategies may expand their applicability. Overall, MXenes represent a versatile platform for photocatalysis and photothermal catalysis, with potential contributions to solar-driven chemical processes at large scale.

Keywords: MXenes; photothermal; 2D nanomaterial; co-catalysts

1. Introduction

Photocatalysis is continuously searching for new processes, materials and mechanisms to break the current ground of the area that is characterized by still insufficient yields and efficiencies [1]. In this search, graphitic carbon nitrides (g-C_3N_4) and other metal-free photocatalysts with 2D morphology have constituted a step forward considering their availability, reliable synthesis and wide range of applications [2]. In 2011, Naguib, Barsoum and Gogotsi reported the preparation of a novel 2D nanomaterial that was termed as MXene [3]. Compared to g-C_3N_4, MXenes offered a considerable wider chemical space since they are constituted by early transitions metals combined with carbon and nitrogen [4] MXene structure is formed by the stacking of one atom thick layer of early transition metals alternating with one atom-thick layer of carbon or nitrogen. The total number of layers can be 3 to 9 and the metal layers are always external, thus resulting in a general formula of $M_{n+1}X_n$, where M is the early transition metal and X is the carbide, nitride or carbonitride layer. Figure 1 summarizes MXene structure for the case of a $M_3X_2O_x$ formula in where -O- are surface terminal groups.

One of the uniqueness of MXenes is that the exposed top and bottom M layers, corresponding to partially oxidized metal, are bonded to surface terminal groups whose nature depends on the preparation process. This surface terminations control many physical, optoelectronic and chemical properties of MXenes, including polarity, hydrophilicity, adsorption energy, work function and others [5]. MXenes exhibit generally high electrical and thermal conductivity, but again, this conductivity depends and can be modulated by the surface terminations as well by the nature of the M transition metal [6,7].

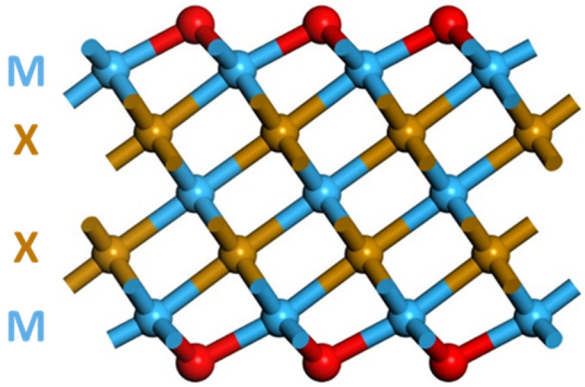

Figure 1. Illustration of five-layers MXene structure in where M (in light bluer) refers to an early transition metal and X (in brown) correspond to carbon or nitrogen. The red atoms correspond to -O- atoms as surface terminations.

Since their discovery, MXenes have found application in energy storage devices such as cathodes for lithium batteries and in supercapacitors, but also in electrocatalysis [8]. MXenes offer also considerable promises in photocatalysis [9,10]. Initial reports were focused on the use of MXenes as cocatalysts, but direct photocatalytic activity of MXenes have also been reported as shown below.

In the broader landscape of 2D materials for photocatalysis, MXenes occupy a distinct yet largely complementary role. Graphene is widely recognized for its excellent electron-accepting capability and outstanding chemical stability, while transition metal dichalcogenides and graphitic carbon nitride function as active semiconductors with tunable bandgaps suitable for visible-light harvesting. In contrast, MXenes combine high metallic conductivity, tunable hydrophilicity, and versatile surface chemistry, making them particularly effective as co-catalysts and conductive scaffolds for promoting interfacial charge transfer in heterojunctions. When integrated with photoactive semiconductors, they can significantly enhance charge separation and suppress recombination processes. In this context, MXenes complement key charge-transfer limitations that often constrain the performance of otherwise well-established photocatalytic systems. The present perspective describes our views in the unique opportunities that MXenes offer on photocatalysis, particularly regarding formation of heterojunctions and photothermal reactions.

2. Synthesis of MXenes

The most general procedures for MXene preparation start with the so-called MAX precursors, in where A corresponds generally to a main group metal of the III and IV groups [3,11]. These MAX precursors can be prepared by metallurgic synthesis by sintering at elevated temperatures of the metallic elements and graphite in the corresponding molar proportions [12]. In the most common cases, the A element is Al, but Ga, Si and As are also possible [12]. Starting from the MAX precursors, MXenes are obtained by chemical etching of the Al element [13]. The two most general etching procedures involve either the use of F-containing etchant in aqueous medium at low temperature or the Lewis acid molten salt etching at temperatures above 450 °C [13,14]. Figure 2 illustrates these two preparation methods.

The etching conditions determine the nature of the surface terminations that become installed on the resulting MXene surface and upon the removal of the A element. In the etching by F-containing reagents, due to the presence of water as solvent not only F but also -O- and -OH are implanted on the surface. These three terminations can be accompanied by other halides, particularly -Cl, if they are present during the etching process. In the case of Lewis acid molten salt etching, since the most general molten salts are alkali metal halides, the corresponding halide is introduced as surface termination during the preparation of the material (Scheme 1) [14].

Surface terminations are important because DFT calculations have shown that the work function and electric conductivity of a given MXene sample are strongly influenced by them [15]. It has been established that Sc carbide with oxygen surface functional groups has a bandgap that should perform as semiconductor, although an experimental validation of the performance of stability of these materials is still missing [16]. In general, and due to the metallic character and electrical conductivity of MXenes, most of these materials do not exhibit semiconducting properties.

However, on the other hand, the metallic character of MXenes and the confinement of valence band electrons on a 2D plane determines the appearance of a plasmon absorption band in the visible region reaching to the near

IR [17]. Therefore, this property makes MXenes promising candidates for plasmonic photocatalysis, enabling photothermal processes in which light is converted into localized heat and hot electrons [18,19]. Figure 3 compares the plasmon band of Ti_3C_2 with that of Au nanoparticles supported on TiO_2.

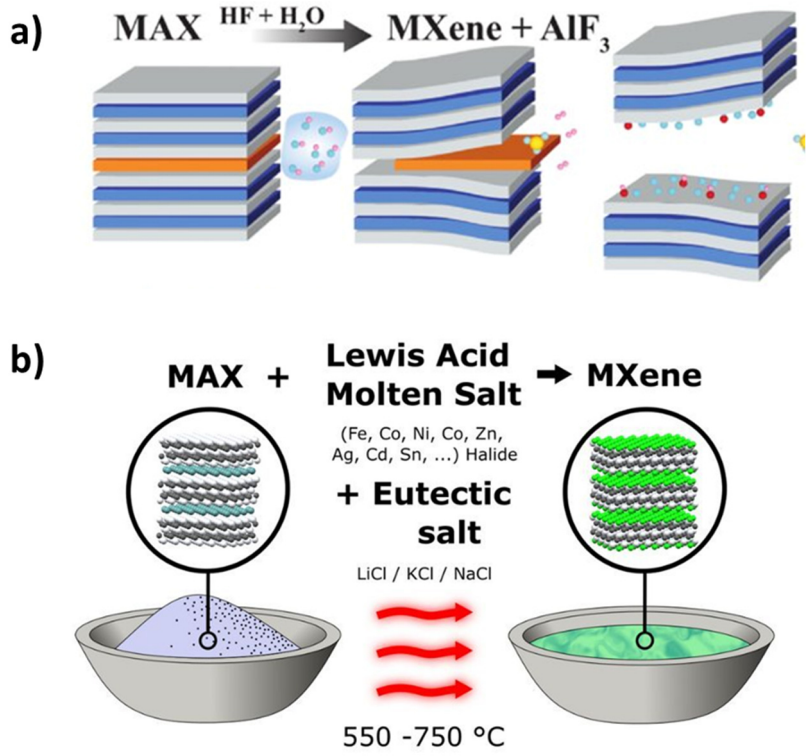

Figure 2. (**a**) HF etching and (**b**) molten salt etching methods for MXene preparation from the corresponding MAX phase precursor.

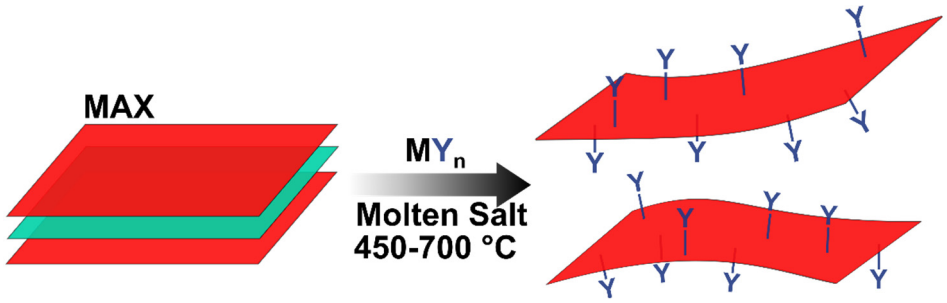

Scheme 1. Spontaneous surface functionalization by halide (Y) of MXenes in molten salt etching preparation.

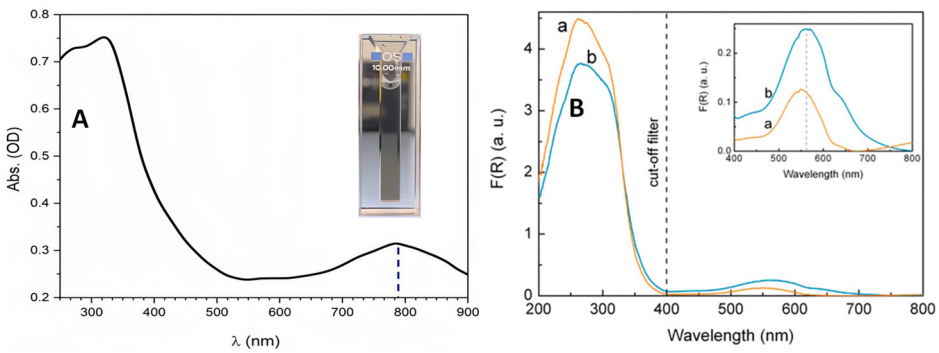

Figure 3. Comparison between plasmon band of Ti_3C_2 and Au nanoparticles supported in TiO_2. Part A UV-Vis absorption spectrum of Ti_3C_2, adapted with permission from ref. [20] under the terms of creative commons attribution license; and Part B, UV-Vis absorption spectra of Au/TiO_2 prepared under 200 (orange) and 400 °C (blue), reproduced with permission from ref. [21]. Copyright 2011 American Chemical Society.

In addition, the metallic character can also be useful for the formation of Schottky heterojunctions, as in the case of noble metal nanoparticles and graphene materials [22]. In these heterojunctions, the electrical conductivity and high charge carrier mobility of the metal nanoparticle facilitates charge migration at the interphase between MXene and the semiconductor and in this way increases efficiency of photoinduced charge separation, decreasing the unproductive electron-hole recombination.

Besides installing surface functional groups that could tune MXene conducting/semiconducting properties, the harsh conditions of the etching can also generate structural defects, and particularly metal atom vacancies that can play diverse roles acting as catalytic sites for substrate adsorption, or favoring substrate reaction or as charge carrier trapping center, among other effects [23]. Therefore, these structural defects can also be beneficial in a photocatalytic process by promoting charge transfer between the MXene and the substrate or by catalyzing substrate transformation after charge transfer.

MXenes are intrinsically susceptible to undergo oxidative degradation, governed by a combination of thermodynamic and kinetic factors and strongly influenced by both environmental conditions and intrinsic material properties. Exposure to water/moisture and dissolved oxygen may initiate oxidation processes, particularly promoted under photocatalytic conditions by photogenerated holes and generation of reactive oxygen species. Surfaces and especially edges are particularly vulnerable to attack, as surface terminations (-O, -OH, -F) can actively participate in reactions with oxygen- and water-derived species [24,25]. In addition to external parameters such as temperature and pH, intrinsic features play a decisive role in determining stability [24]. Defects such as metal and carbon vacancies act as highly reactive sites that facilitate water adsorption and protonation, lowering activation barriers for bond cleavage and promoting metal atom release [26]. Experimental studies have further revealed stepwise degradation pathways involving loss of surface functional groups, structural rearrangement, and the formation of oxide phases such as TiO_2, confirming the progressive transformation of the MXene lattice [26]. To mitigate these effects, several strategies have been proposed, including surface and edge passivation via ligand interactions, protective coatings, defect passivation, and hybridization with semiconductors, which can suppress degradation by limiting access of reactive species and tuning the electronic structure [24,25]. Moreover, the practical applicability of MXenes in photocatalytic systems is frequently compromised by the restacking tendency of their nanosheets which results in a drastic reduction of specific surface area and the obstruction of catalytically active sites [27]. This aggregation process is further intensified by capillary forces inherent to conventional drying and processing methods, which trigger porosity collapse and hinder mass transport. Consequently, these structural limitations prevent the material from achieving its theoretical performance in reactions that depend on highly accessible and well-exposed surfaces [28,29].

3. MXenes as Co-Catalysts to Enhance the Photocatalytic Activity of Dyes and Semiconductors

One of the pioneering studies on the applicability of MXenes in photocatalysis was the use of MXenes as cocatalyst replacing Pt nanoparticles in photoinduced hydrogen evolution reaction (HER) (Scheme 2) [30]. In this study, Eosin Y was used as light harvester and sensitizer due to the intense absorption of this dye in the visible region. Organic dyes meet well one of the most important prerequisites in photocatalysis regarding the ability to absorb photons and generate electronic excited states. However, these organic compounds typically fall short in promoting chemical transformations on substrates, such as hydrogen evolution, due to their lack of activity for gas evolution. For this reason, organic sensitizers must be combined with other materials acting as co-catalysts, with noble metal nanoparticles being among the most widely used option [31]. However, the excessive cost and scarcity of noble metals make convenient their replacement by more affordable alternatives. In this regard it is also reported that addition of MXenes to Eosin Y using methanol as sacrificial hole scavenger can promote HER upon visible light irradiation, reaching a H_2 production of 33.4 μmol g_{cat}^{-1} h^{-1}.

Following with this research, we have shown that the efficiency of MXenes as co-catalysts for HER under visible light irradiation increases with the degree of exfoliation of the MXene [32]. Typically, surface area is measured using dry powders by N_2 gas absorption. These measurements give, in the case of MXenes, small specific surface area values about a few $m^2 \times g^{-1}$. As in the case of other 2D nanomaterials this small area values are mostly due to the lack of intrinsic porosity of MXenes that undergo stacking under dry conditions. In contrast, in liquid suspensions, upon sonication the exposed surface area of exfoliated few-layers MXene platelets can be much larger than the value indicated by N_2 absorption. Using the Aksay method based on formation of a monolayer of methylene blue coating Nb_2C platelets suspended in aqueous phase, surface area values as large as 100 m^2/g were estimated for Nb_2C in aqueous suspension [32]. A favorable relationship between Nb_2C surface area, as determined by the methylene blue adsorption method in suspended particles, and HER activity of 10.3 mmol g_{cat}^{-1} h^{-1} was

observed for Nb_2C as co-catalyst using Eosin Y as photosensitizer and triethanolamine as sacrificial electron donor. Scheme 3 illustrates the proposed mechanism for this process.

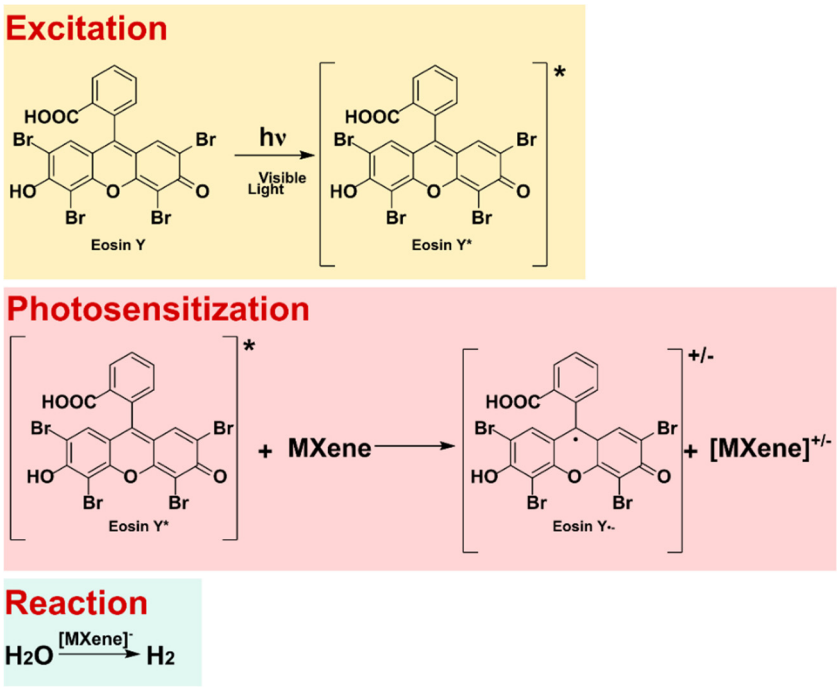

Scheme 2. MXenes as co-catalysts for Eosin Y photosensitization in HER.

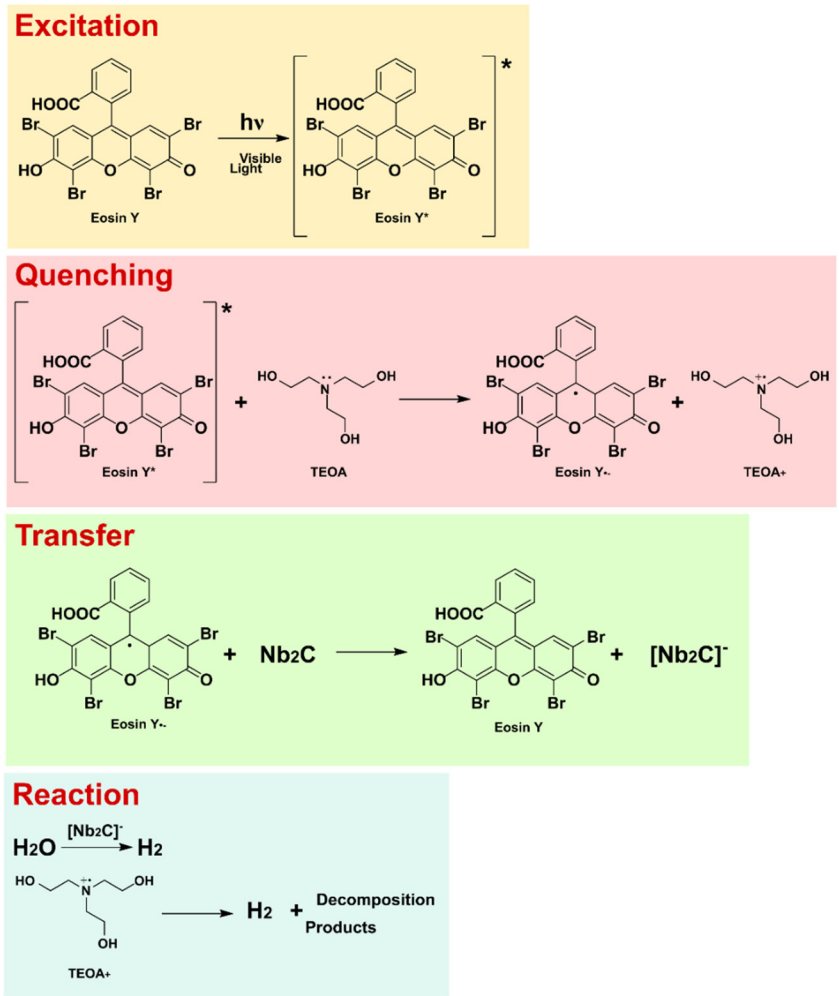

Scheme 3. Proposed mechanism for HER in Nb_2C using Eosin Y as photosensitizer and triethanolamine as sacrificial electron donor.

In a further realization of MXenes as cocatalysts, it was also found that Nb_2C as co-catalyst together with Co(II) salt in solution increase the HER efficiency of Eosin Y photosensitizer using triethanolamine (TEOA) as sacrificial electron donor, producing H_2 at a 10.3 mmol g_{cat}^{-1} h^{-1} rate [33]. It has to be commented that organic dyes as photosensitizer can reach very high quantum efficiency values for HER and other photocatalytic reactions, reaching apparent quantum efficiencies over 15%, that are values rarely reported for solid semiconductors and are clearly remarkable and worth to be exploited [34,35].

4. MXene Dots as Semiconductors

As previously commented, most of the MXene samples are electrically conductive and therefore, these samples can be adequate for the use of MXenes as cocatalysts, but the lack of an energy gap between the valence and the conduction bands precludes their use as semiconductors. In fact, the use of MXenes as electrocatalysts takes advantage of having simultaneously an electrically conductive material and active metallic sites that are able to promote chemical transformations [36]. However, this in-plane electrical conductivity is mostly due to the large lateral surface area of MXenes samples, frequently with particle sizes well over 100 nm^2.

As in the case of quantum dots, carbon dots and other nanomaterials, confinement effects can open a gap between the conduction and the valence band [37]. This is apparently the case of MXene dots, in where the lateral dimension is in the order of tens of nm [38,39]. Thus, by reducing the lateral size, MXene can become semiconductors due presumably to quantum confinement effects. This semiconducting properties of MXene dots are reflected in their optical absorption and the appearance of an emission spectrum. Calculations should determine the influence of lateral size, nature of the surface terminations on the energy position of the valence and conduction bands.

Among the various ways to obtain them [38], quantum dots can be formed directly from the MAX phase precursor by liquid phase laser ablation [40]. In this method, a short laser pulse hitting suspended MAX particles produces a mechanical and thermal shock in the MAX crystal structure as result of the instantaneous transfer of energy and momentum of the laser beam on to the particle surface.

These energy pulses cause the etching of the A element that becomes oxidized and removed from the structure. and the formation of MXene nanoparticles. Liquid laser ablation to obtain MXene dots has the advantage to be a physical etching method not requiring chemical etchants, particularly avoiding HF or any fluoride salt. The solvent in which the ablation is made determines the nature of the resultant surface functionalization. Scheme 4 illustrates the generation of MXene dots upon irradiation of the MAX precursor in aqueous phase [41].

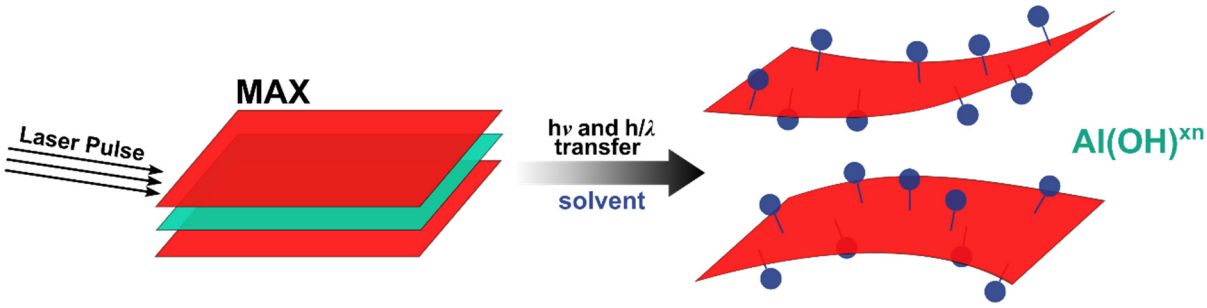

Scheme 4. Liquid laser ablation of MAX phase forming MXene dots due to the transfer in submicrosecond time scale of energy (*hn*) and momentum (*h/l*). Deep blue spheres represent the groups attached on the MXene dot from the alcohol medium.

Evidence of the MXene structure of these small nanoparticles formed in the laser ablation is obtained by TEM showing the morphology and crystallinity of the dots, XRD pattern corresponding to the MXene phase and XPS providing information of the composition and coordination of the nanoparticles, among other characterization techniques. It was found that theses MXene dots in the absence of light harvesting dyes or semiconductors can promote upon irradiation with simulated sunlight photocatalytic hydrogen evolution, oxygen evolution and even overall water splitting in the absence of any sacrificial electron donor or acceptor agent [41,42].

Interestingly, it was found that the photocatalytic activity (2.02 mmol g_{cat}^{-1} h^{-1}) increases upon reuse of the same sample in consecutive runs, a fact that has been explained as arising from the variation of the surface functional groups upon prolonged irradiation [41]. Figure 4 presents some of the results reported for these MXenes nanoparticles.

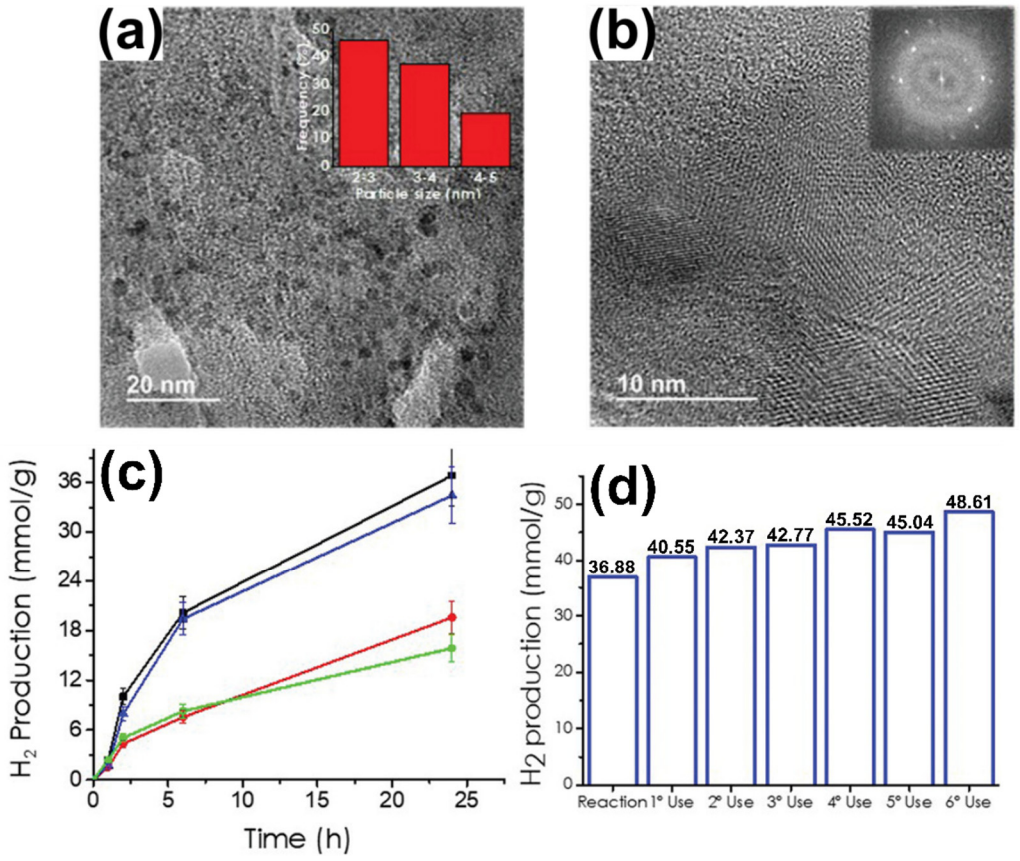

Figure 4. (**a**,**b**) TEM images of Ti_3AlC_2 quantum dots obtained by laser ablation method in H_2O as solvent. Statistical particle size gives an average size of 5 nm, (**c**) Photocatalytic H_2 evolution reaction curve for (■) Ti_3C_2; (▼) Nb_2C; (●) Ti_2C; and (◊) V_2C dots obtained by laser ablation (532 nm, 7 ns pulse, 50 mJ × $pulse^{-1}$) of the corresponding MAX phases (A = Al) in H_2O suspension; and (**d**) reuses of Ti_3C_2 dot. Reaction conditions: 1 mg of MXene dot in milli Q water containing triethanolamine upon irradiation with 300 W Xe lamp with l < 400 nm cut-off filter. Taken with permission from ref. [41] under the terms of creative commons attribution license.

Besides photocatalytic HER and overall water splitting, MXenes dots obtained by laser ablation have been also found to be active for photocatalytic CO_2 hydrogenation to CH_4 (891 μmol g_{cat}^{-1} h^{-1}). Figure 5 presents some of the results published for CO_2 reduction [42].

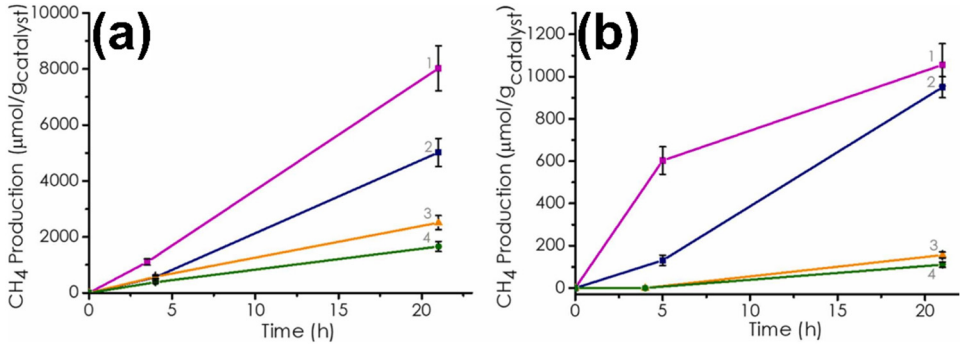

Figure 5. Temporal profile of CO_2 to CH_4 photocatalytic hydrogenation results for Ti_3C_2 (pink), Nb_2C (blue), V_2C (yellow) and Ti_2C (green) MXene nanoparticles upon (**a**) UV-Vis irradiation and (**b**) visible (λ > 400 nm) light. Reproduced from ref. [42] under the terms of creative commons attribution license.

Besides H_2O, MXene dots can also be formed upon liquid phase ablation in alcohols as solvents. In these cases, IR spectroscopy has provided compelling evidence that the surface functionalities occurring on the MXene dots are related to the structure of the alcohol in which irradiation is carried out (Figure 6) [42]. As expected, based on the knowledge on the influence of surface functional groups on MXene properties, it was also found that the photocatalytic activity of these MXene dots depends on the surface functionality introduced in the process and therefore in the alcohol used in the laser ablation.

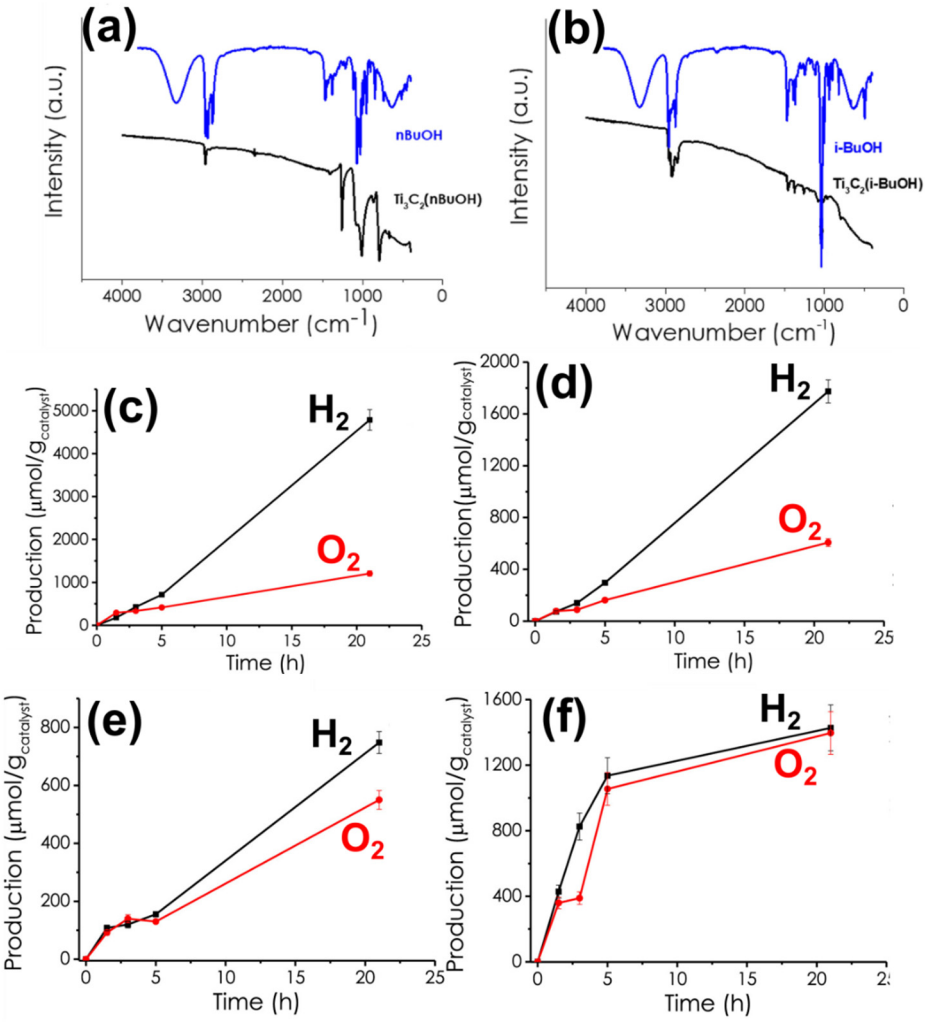

Figure 6. (**a**) FTIR spectra of Ti_3C_2(nBuOH) and n-BuOH for comparison (**b**) FTIR spectra of Ti_3C_2(*i*-BuOH) and *i*-BuOH for comparison and H_2 and O_2 production obtained from photocatalytic water splitting reaction for (**c**) Ti_3C_2(EtOH + TBAOH), (**d**) Ti_3C_2(CF_3CH_2OH), (**e**) Ti_3C_2(n-$C_8H_{17}OH$) and (**f**) Ti_3C_2(TBAOH + H_2O). The brackets indicate the alcohol in which the laser ablation was made. Reproduced with permission from ref. [42] under the terms of creative commons attribution license.

It can be expected that laser ablation will be particularly useful to obtain MXene samples that are difficult to prepare by conventional etching methods. In this regard, laser ablation could be specially interesting to prepare MXene nitrides that are almost impossible to be obtained by fluoride etching or by molten salt methods, but they could be in principle prepared by laser ablation under adequate conditions regarding laser wavelength and power, pulse duration, solvent and others. MXene nitrides could have the general advantage of offering larger stability than MXene carbides [43,44]. In fact, in most of the photocatalytic hydrogen evolution experiments previously commented, evolution of CO_2 and CH_4 has been observed, therefore indicating the lack of complete photocatalytic stability of MXene dots. As commented earlier, MXenes are particularly prone to undergo oxidation and it can be expected that this tendency will be even more facilitated when the lateral size is small as consequence of the increased prevalence of peripheral atoms. This issue of MXene dot stability certainly merits a detailed study trying to develop efficient methods to minimize this unwanted process.

5. MXenes Heterojunctions

One of the main advantages of 2D nanomaterials is the large percentage of atoms that can be accessible to substrates and products. 2D morphology is also especially suitable to expose a large interface to other 2D nanomaterials or nanoparticles [45].

The combination of two materials can increase the efficiency of a photocatalytic process. In fact, one of the main bottlenecks of a photocatalysis is charge recombination after photon excitation and generation of photoinduced charge separation. Due to fast and efficient charge recombination it is a general observation that the

junction of two semiconductors with appropriate band alignment is more efficient in photocatalysis than a single material [46]. In a heterojunction at least one semiconducting material establishes and interfacial contact with other conductive or semiconducting material.

This intimate contact makes possible after photoexcitation charge carrier migration from one component to the other. The charge migration is mainly driven by the creation at the interface of a built-in internal electric field (IEF) due to differences in the work function between the two components as indicated in Scheme 5.

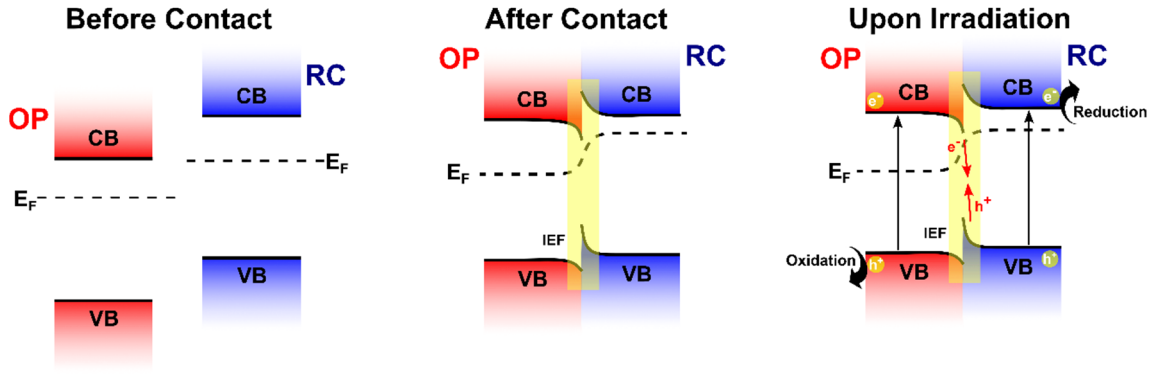

Scheme 5. Illustration of a S-scheme heterojunction between 2D semiconductors. CB, E_F, VB, IEF, OP and RP correspond to conduction band, Fermi level, valence band, internal electric field, oxidizing photocatalyst and reduction photocatalyst, respectively.

One prerequisite for an efficient heterojunction is to have a large interfacial contact and favorable electron paths between the two materials. Accordingly, MXenes appear to be suitable materials for forming heterojunctions since they can provide an interface involving a considerable proportion of atoms forming the material and surface functional groups can provide a path for charge carrier migration at the interface. In addition, the high electrical conductivity of MXenes should also favor charge mobility and migration.

One of the examples of MXene heterojunctions in photocatalysis is the combination of g-C_3N_4, a semiconductor, with Ti_3C_2. The heterojunction was assembled by electrostatic attraction between previously protonated g-C_3N_4 with positive surface charge and the Ti MXene. The formation of the heterojunction increases the photocatalytic activity of hydrogen evolution in the presence of 10% of triethanolamine as sacrificial electron donor by a factor of 10 compared to the activity of g-C_3N_4 having 3% of Pt, showing H_2 evolution rate of 72.3 μmol g_{cat}^{-1} h^{-1} under best conditions [47].

In another example of MXene heterojunction, we have prepared a 2D Cu porphyrin MOF on Ti_3C_2 MXene by ultrasonication of preformed materials and observed an increase in the photocatalytic overall H_2O splitting of the heterojunction in comparison to the activity of supported Cu porphyrin MOF (Figure 7**)** [48]. The formation of the heterojunction provided a material able to perform a catalytic activity for H_2 production of 1.67 mmol g_{cat}^{-1} h^{-1}.In this case, generation of an internal electric field at the interface was supported by XPS that shows an enrichment of electron density in Cu 2p and a decrease of electron density in Ti 2p core levels after formation of the heterojunction, while in situ irradiated XPS shows shifts in the opposite direction indicating charge migration at the interface from MXene to the 2D Cu porphyrin MOF. Interestingly, the lower than stoichiometric amount of O_2 formed respect to H_2 in the overall water splitting experiment was accompanied by observation of CO_2 evolution, thereby indicating the lack of complete stability of Ti_3C_2 that should undergo self-oxidation by photogenerated holes [48]. This would suggest that MXenes are better suited to act in a heterojunction as reduction photocatalyst, since their stability as oxidation photocatalyst can be limited.

It can be expected that MXenes will be used as preferent materials in many other heterojunctions involving typical metal oxides or sulphides semiconductors. In fact, spontaneous or forced partial oxidation of MXenes can form in situ a heterojunction of the corresponding oxide of the transition metal present in the MXene and the MXene itself. This in situ synthesis establishes a good interface that results generally in an enhanced photocatalytic activity for HER, CO_2 reduction and pollutant degradation.

In this regard, the combination of TiO_2 and Ti_3C_2 has been one of the first and so far better studied metal oxide/MXene heterojunctions [49–53]. As illustrated in Scheme 6, these metal oxides on MXene can be conveniently obtained by hydrothermal oxidation of the MXene in aqueous medium containing high ionic strength. The *in-situ* growth creates an interface suited to promote an efficient charge migration between the two components, favoring CO_2 to CH_4 production rate of 4.4 mmol g_{cat}^{-1} h^{-1} under optimal conditions [50]. Other

preferred heterojunctions are the Nb_2O_{5-x} over Nb_2C that is efficient for photocatalytic CO_2 reduction. The material obtained achieves a CO and CH_4 production rate of 1.24 and 2.04 μmol g_{cat}^{-1} h^{-1}, respectively [54,55].

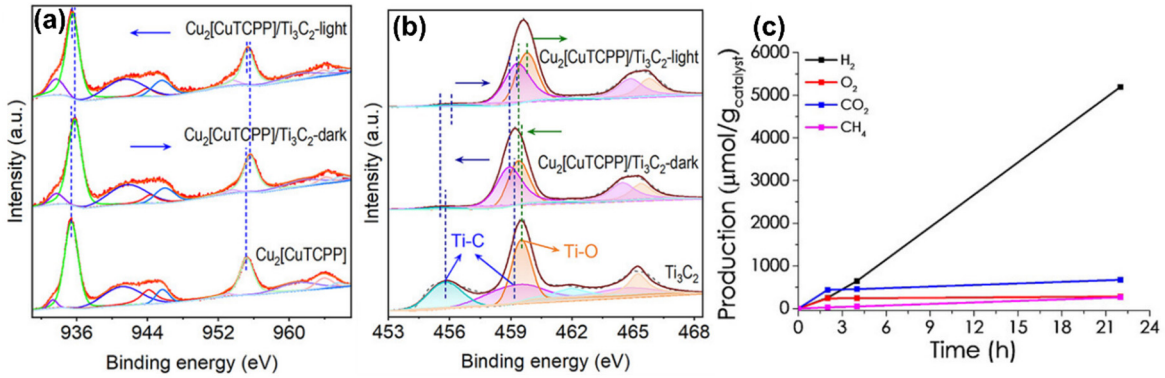

Figure 7. *In situ* irradiated high-resolution XPS data recorded in Cu_2[CuTCPP]/Ti_3C_2 (TCPP: *meso*-tetrakis(carboxyphenyl)porphyrin) for (**a**) Cu 2p and (**b**) Ti 2p core levels and (**c**) photocatalytic overall H_2O splitting observing together with H_2 and O_2, the formation of CO_2 and CH_4. Taken with permission from ref. [48].

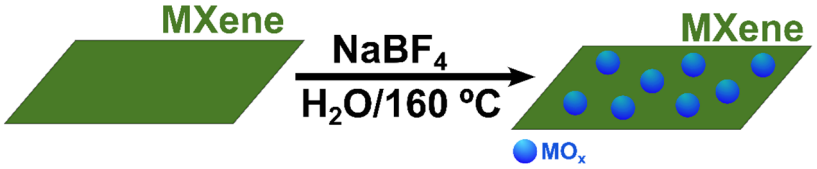

Scheme 6. *In situ* growth of MOx/MXene heterojunction by partial oxidation of MXene.

From a mechanistic perspective, different types of MXene-based heterojunctions should exhibit distinct charge transfer behavior that directly impact photocatalytic performance. In Schottky heterojunctions, the metallic character of MXenes prevails and they act as electron sinks, favoring charge separation via electron trapping and suppressing recombination. In contrast, S-scheme heterojunctions rely on a built-in electric field and band bending to selectively recombine low-energy electrons on the oxidizing semiconductor with low-energy holes located at the reducing photocatalyst, thereby preserving highly reactive electrons and holes with the strongest redox potentials. Although both approaches can enhance photocatalytic activity, direct comparisons of their efficiencies remain challenging due to differences in experimental conditions across studies.

6. MXenes as Photothermal Catalysts

Typical photocatalytic activity involves charge separation with the generation of conduction band electrons and valence band holes upon photon absorption. However, particularly in plasmonic materials, a new mechanism, still not totally understood, termed as photothermal process has recently been considered [18,19,56,57]. This mechanism combines activation by heat and light opening new pathways in which reaction intermediates are submitted not only to heat as in thermal catalysis, but also to the action of hot electrons and electric fields (Scheme 7) [18]. In these systems, light absorption can generate highly energetic charge carriers such as conduction band electrons and holes, but also hot electrons which, in addition of generating local electric fields may be transferred to electron-accepting orbitals of adsorbed species, promoting the reactivity of reaction intermediates through electronic or vibrational excitation and enabling easier bond weakening or cleavage of these intermediates in comparison to the conditions of the purely thermal reactions [18].

Frequently instead of external heating, light, particularly, of the near IR region is used to increase the temperature, these long-wavelength photons becoming thermalized and converted into heat by photon/phonon conversion [57]. This novel photothermal mechanism has been frequently observed in plasmonic materials, often composed by metal nanoparticles or metal-metal oxides particles [18].

MXenes exhibit high electrical and thermal conductivity. The confinement in the vertical direction and their metallic character results in the appearance of a plasmonic absorption band in the red region of the visible zone expanding to the near-IR region (Figure 3). MXenes have been reported as being very efficiency for the conversion of solar light into heat, reaching estimated efficiencies over 90% [58,59]. Therefore, MXenes appear to be especially suited to promote photothermal reactions. In addition, MXenes can also support some metal overlayers that also contribute to the photothermal mechanism or introduce catalytic activity.

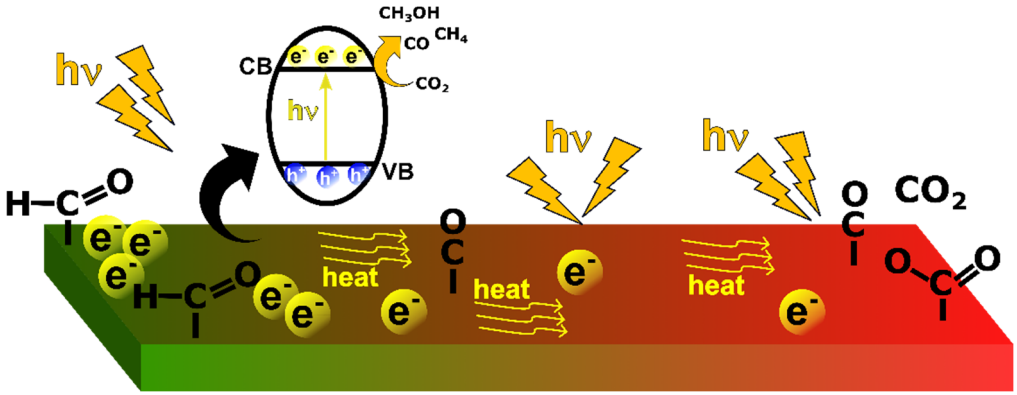

Scheme 7. Illustration of the photothermal mechanism with the simultaneous operation of temperature gradient, electric fields and hot electrons on the reaction intermediates appearing in CO_2 reduction.

It has been reported that the activation barriers occurring in thermal catalysis become lower when the reaction intermediate and transitions states experience the effect of a light-induced charge redistribution [60]. Analogously, reduction potentials of reaction intermediates involved in a genuine photoinduced charge separation mechanism are decreased according to the Nernst equation when the temperature increases. In other words, the reaction intermediates can be similar in photothermal and thermal mechanism, but require lesser temperatures or lower reduction potential when the process is carried out under the combined energy input of heat and light.

In one of the examples in the literature regarding the use of MXenes as photothermal catalysts, $Ti_3C_2Cl_2$ obtained by the molten salt method having Ni particles was used. The Ni-$Ti_3C_2Cl_2$ sample forms in a single step during the Lewis acid molten salt etching of Ti_2AlC_2 by $NiCl_2$ in NaCl/KCl eutectic mixture [61].

Characterization of these Ni-$Ti_3C_2Cl_2$ by XRD shows that the interaction between Ti and Ni derived from the synthesis conditions is so strong that at the interface appears a metal Ni_3Ti alloy detectable by XRD. These Ni/$Ti_3C_2Cl_2$ samples upon irradiation plus external heating at 200 °C are able to form CH_3OH when the system is submitted to a pression of 20 bars, reaching 1300 and 6.8 μmol g_{cat}^{-1} h^{-1} production rates for CH_4 and CH_3OH, respectively, under optimized condition. In comparison, the thermal activity of the same material in the dark is negligible, thus proving the effect of light in the reaction. Figure 8 illustrates some of the results of the photothermal CO_2 hydrogenation over Ni/$Ti_3C_2Cl_2$.

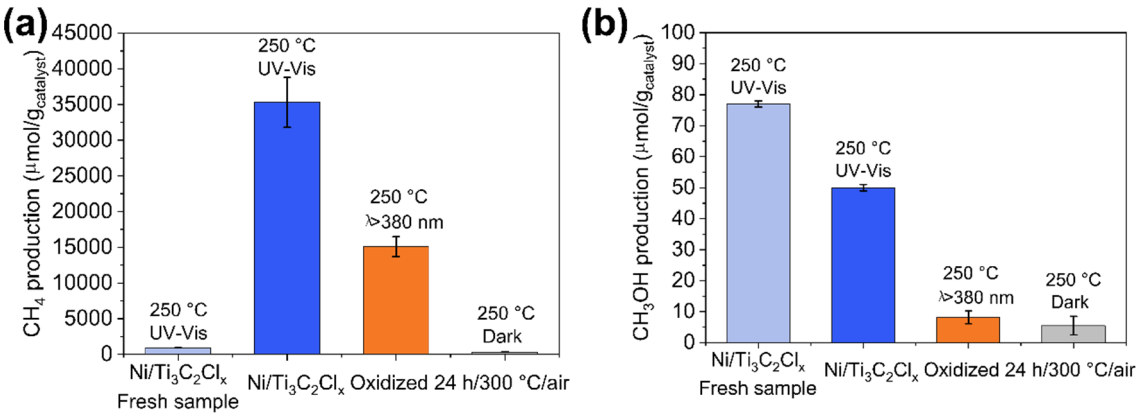

Figure 8. (**a**) CH_4 and (**b**) CH_3OH production in photothermal CO_2 catalytic reduction using Ni/$Ti_3C_2Cl_2$ under different conditions. Reproduced with permission from ref. [61] under the terms of Creative Commons Attribution license.

Considering the properties of MXenes as plasmonic materials and the thermal stability allowing to heat at temperatures below 700 °C under reductive conditions, it can be expected that these 2D nanomaterials will be widely used for photothermal hydrogenations, including CO_2 reduction and N_2 fixation, as well as other types of light-enhanced thermal reactions.

7. Conclusions and Future Perspectives

MXenes are relatively new to 2D nanomaterials that have attracted increasing interest in many applications related to energy storage, as well as in thermal and electrocatalysis. The unique properties of MXenes in terms of

chemical composition, tunable surface groups, electrical and thermal conductivities, 2D morphology and others offer also considerable promises in photocatalysis. Since the initial studies showing the possibility to substitute Pt nanoparticles by MXenes, the use of MXenes in photocatalysis has continuously expanded, showing not only the photocatalytic activity of MXene dots, but also the considerable opportunity to apply MXenes for efficient heterojunctions with other materials. The conducting or semiconducting properties of MXenes are well suited to stablish Schottky barriers or S-scheme heterojunctions with semiconductors. Some of these heterojunctions can be obtained by sacrificial partial oxidation or modification of MXenes, while in other cases electrostatic attraction or in situ synthesis can be applied to obtain the second component on the MXene. These heterojunctions have as bottleneck the unsatisfactory stability of MXene carbides against oxidation. This drawback could be overcome by employing MXenes nitrides that should be comparatively more stable than carbides or by tuning the work function of the MXene in a way that photogenerated holes remain in the other component and MXenes perform the role of reduction photocatalyst. For this type of heterostructures, MXenes offer a unique platform to also incorporate other active sites and particularly single atoms that can further improve productivity by acting as catalytic sites. MXenes are also very appropriate materials for light to heat conversion that can be applied in photothermal reactions. For this reaction type generally requiring plasmonic absorption, as well as thermal and electrical conductivity, the properties of MXenes fit particularly well. In fact, MXenes can reach under 1 Sun-power illumination very high temperatures, probably among the highest for any material [57]. In addition, MXenes undergo at the same time optoelectronic phenomena related to charge migration and generation of hot electrons. Therefore, photothermal is an area expected to grow in the near future with particular emphasis in photothermal CO_2 conversion and N_2 fixation. Looking ahead, future progress in MXene-based photocatalysis will rely on the development of more controlled and scalable strategies to overcome current key limitations. In particular, selective surface termination engineering, together with post-synthesis chemical modifications, provide effective routes to finely tune their electronic structure and catalytic performance. In parallel, recent advances in etching protocols, the use of greener precursors and methods, and more reproducible delamination strategies are essential to enable scalable and consistent material production. In this way, these approaches are expected to bridge the gap between fundamental understanding and practical applications of MXenes in photocatalysis.

Overall, the present perspective illustrates the current interest on MXenes in the field of photocatalysis due to the unique MXene properties that complement those of other known photocatalysts. It can be expected that MXenes will be increasingly used in photocatalysis and can improve the performance or even open new reaction mechanisms that could serve to achieve the long-standing goal of modern photocatalysis, namely, the utilization of natural sunlight to obtain renewable fuels or implement chemical processes at a large scale, contributing to in this way to decarbonization and mitigation of the climate change.

Author Contributions

G.H.C.d.S: Conceptualization, Methodology, Visualization, Writing—original draft, Writing—review & editing; H.G.: Conceptualization, Funding acquisition, Methodology, Project administration, Supervision, Writing—original draft, Writing—review & editing; A.P.: Conceptualization, Funding acquisition, Methodology, Project administration, Writing—review & editing. All authors have read and agreed to the published version of the manuscript.

Funding

Financial support by the Spanish Ministry of Science and Innovation (CEX-2021-001230-S and PID2024-161014 NB-I00 funded by MCIN/AEI/10.13039/501100011033), Generalitat Valenciana (CIPROM/2024/071) and European Commission through the ERC Adv. Grant 101141466 DISCOVERY is gratefully acknowledged.

Conflicts of Interest

The authors declare no conflict of interest. Given the role as Editor-in-chief, Hermenegildo García had no involvement in the peer review of this paper and had no access to information regarding its peer-review process. Full responsibility for the editorial process of this paper was delegated to another editor of the journal.

Use of AI and AI-Assisted Technologies

No AI tools were utilized for this paper.

References

1. Fresno, F.; Portela, R.; Suárez, S.; et al. Photocatalytic materials: Recent achievements and near future trends. *J. Mater. Chem. A* **2014**, *2*, 2863–2884.
2. Cao, S.; Low, J.; Yu, J.; et al. Polymeric photocatalysts based on graphitic carbon nitride. *Adv. Mater.* **2015**, *27*, 2150–2176.
3. Naguib, M.; Kurtoglu, M.; Presser, V.; et al. Two-dimensional nanocrystals: Two-dimensional nanocrystals produced by exfoliation of Ti_3AlC_2 (Adv. Mater. 37/2011). *Adv. Mater.* **2011**, *23*, 4207.
4. Li, X.; Huang, Z.; Shuck, C.E.; et al. MXene chemistry, electrochemistry and energy storage applications. *Nat. Rev. Chem.* **2022**, *6*, 389–404.
5. Mozafari, M.; Soroush, M. Surface functionalization of MXenes. *Mater. Adv.* **2021**, *2*, 7277–7307.
6. Liu, Y.; Wu, Y.; Wang, X. Thermal transports in the MXenes family: Opportunities and challenges. *Nano Res.* **2024**, *17*, 7700–7716.
7. Hantanasirisakul, K.; Gogotsi, Y. Electronic and optical properties of 2D transition metal carbides and nitrides (MXenes). In *Mxenes*; Jenny Stanford Publishing: New York, NY, USA, 2023; pp. 135–205.
8. Pang, J.; Mendes, R.G.; Bachmatiuk, A.; et al. Applications of 2D MXenes in energy conversion and storage systems. *Chem. Soc. Rev.* **2019**, *48*, 72–133.
9. Murali, G.; Reddy Modigunta, J.K.; Park, Y.H.; et al. A review on MXene synthesis, stability, and photocatalytic applications. *ACS Nano* **2022**, *16*, 13370–13429.
10. Li, Y.; Chen, X.; Sun, Y.; et al. Chlorosome-Like Molecular Aggregation of Chlorophyll Derivative on $Ti_3C_2T_x$ MXene Nanosheets for Efficient Noble Metal-Free Photocatalytic Hydrogen Evolution. *Adv. Mater. Interfaces* **2020**, *7*, 1902080.
11. Naguib, M.; Barsoum, M.W.; Gogotsi, Y. Ten years of progress in the synthesis and development of MXenes. *Adv. Mater.* **2021**, *33*, 2103393.
12. Sokol, M.; Natu, V.; Kota, S.; et al. On the chemical diversity of the MAX phases. *Trends Chem.* **2019**, *1*, 210–223.
13. Sun, M.; Chu, S.; Sun, Z.; et al. A review of etching methods and applications of two-dimensional MXenes. *Nanotechnology* **2024**, *35*, 382003.
14. Kruger, D.D.; García, H.; Primo, A. Molten salt derived MXenes: Synthesis and applications. *Adv. Sci.* **2024**, *11*, 2307106.
15. Yusupov, K.; Björk, J.; Rosen, J. A systematic study of work function and electronic properties of MXenes from first principles. *Nanoscale Adv.* **2023**, *5*, 3976–3984.
16. Balcı, E.; Akkuş, Ü.Ö.; Berber, S. Band gap modification in doped MXene: Sc_2CF_2. *J. Mater. Chem. C* **2017**, *5*, 5956–5961.
17. Guo, X.; Li, N.; Wu, C.; et al. Studying plasmon dispersion of MXene for enhanced electromagnetic absorption. *Adv. Mater.* **2022**, *34*, 2201120.
18. Mateo, D.; Cerrillo, J.L.; Durini, S.; et al. Fundamentals and applications of photo-thermal catalysis. *Chem. Soc. Rev.* **2021**, *50*, 2173–2210.
19. Song, C.; Wang, Z.; Yin, Z.; et al. Principles and applications of photothermal catalysis. *Chem Catal.* **2022**, *2*, 52–83.
20. Zaheer, A.; D'Aponte, T.; Babar, Z.U.; et al. One-Step Synthesis of Robust 2D Ti_3C_2-MXene/AuNPs Nanocomposite by Electrostatic Self-Assembly for (Bio)Sensing. *Eng. Proc.* **2023**, *56*, 227. https://doi.org/10.3390/ASEC2023-15227.
21. Gomes Silva, C.; Juárez, R.; Marino, T.; et al. Influence of excitation wavelength (UV or visible light) on the photocatalytic activity of titania containing gold nanoparticles for the generation of hydrogen or oxygen from water. *J. Am. Chem. Soc.* **2011**, *133*, 595–602.
22. Wang, H.; Zhang, L.; Chen, Z.; et al. Semiconductor heterojunction photocatalysts: Design, construction, and photocatalytic performances. *Chem. Soc. Rev.* **2014**, *43*, 5234–5244.
23. Gouveia, J.D.; Gomes, J.R.B. Structural and energetic properties of vacancy defects in MXene surfaces. *Phys. Rev. Mater.* **2022**, *6*, 024004.
24. Kumar, S.; Kumari, N.; Singh, T.; et al. Shielding 2D MXenes against oxidative degradation: Recent advances, factors and preventive measures. *J. Mater. Chem. C* **2024**, *12*, 8243–8281.
25. Khalid, Z.; Hadi, F.; Xie, J.; et al. The future of MXenes: Exploring oxidative degradation pathways and coping with surface/edge passivation approach. *Small* **2025**, *21*, 2407856.
26. Stratulat, A.-M.; Nesterova, V.; Korostelev, V.; et al. Defect-Driven Degradation of MXenes in Aqueous Environments and Mitigation Strategies: Insights from First-Principles. *ACS Nano* **2025**, *19*, 36994–37003.
27. Ahmed, M.A.; Mahmoud, S.A.; Mohamed, A.A. Insights into MXene-based materials for environmental applications: Performance, mechanisms, and future directions. *FlatChem* **2025**, *50*, 100825.
28. Xiu, L.; Wang, Z.; Yu, M.; et al. Aggregation-resistant 3D MXene-based architecture as efficient bifunctional electrocatalyst for overall water splitting. *ACS Nano* **2018**, *12*, 8017–8028.
29. Wang, K.; Hussain, I.; Singh, K.; et al. Fabrication of MXene films through various techniques: A mini review. *Nanoscale* **2025**, *17*, 15676–15689.

30. Sun, Y.; Sun, Y.; Meng, X.; et al. Eosin Y-sensitized partially oxidized Ti_3C_2 MXene for photocatalytic hydrogen evolution. *Catal. Sci. Technol.* **2019**, *9*, 310–315. https://doi.org/10.1039/C8CY02240B.
31. Alotabi, A.S.; Adnan, R.H.; Almutairi, A.M.; et al. A Comprehensive Review of the Role of Overlayers in Photocatalytic Overall Water Splitting and Related Reactions. *Chem. Rev.* **2026**, *126*, 2801–2845.
32. Grau, R.R.; Lewandowska-Andralojc, A.; Primo, A.; et al. Enhancement of the photocatalytic hydrogen production with the exfoliation degree of Nb_2C cocatalyst. *Int. J. Hydrogen Energy* **2023**, *48*, 20314–20323.
33. Smirnova, M.; Scheibe, B.; Ramírez-Grau, R.; et al. Synergistic effects of MXene support and cobalt salts in dye-sensitized photocatalytic hydrogen generation. *Int. J. Hydrogen Energy* **2024**, *88*, 1098–1107.
34. Wilkinson, F.; Helman, W.P.; Ross, A.B. Quantum yields for the photosensitized formation of the lowest electronically excited singlet state of molecular oxygen in solution. *J. Phys. Chem. Ref. Data* **1993**, *22*, 113–262.
35. Baptista, M.S.; Cadet, J.; Greer, A.; et al. Photosensitization reactions of biomolecules: Definition, targets and mechanisms. *Photochem. Photobiol.* **2021**, *97*, 1456–1483.
36. Bai, X.; Guan, J. MXenes for electrocatalysis applications: Modification and hybridization. *Chin. J. Catal.* **2022**, *43*, 2057–2090.
37. Zhang, Y.; Ma, D.; Li, J.; et al. Confinement effects in photocatalysis: Progress and challenges. *J. Mater. Chem. A* **2025**, *13*, 10431–10450.
38. Deng, H.; Hui, Y.; Zhang, C.; et al. MXene−derived quantum dots based photocatalysts: Synthesis, application, prospects, and challenges. *Chin. Chem. Lett.* **2024**, *35*, 109078.
39. Sharbirin, A.S.; Akhtar, S.; Kim, J. Light-emitting MXene quantum dots. *Opto-Electron. Adv.* **2021**, *4*, 200077.
40. Semaltianos, N.G. Nanoparticles by laser ablation. *Crit. Rev. Solid State Mater. Sci.* **2010**, *35*, 105–124.
41. Ramírez, R.; Melillo, A.; Osella, S.; et al. Green, HF-free synthesis of MXene quantum dots and their photocatalytic activity for hydrogen evolution. *Small Methods* **2023**, *7*, 2300063.
42. Ramírez-Grau, R.; Cabrero-Antonino, M.; García, H.; et al. MXene dots as photocatalysts for CO_2 hydrogenation. *Appl. Catal. B: Environ.* **2024**, *341*, 123316.
43. Zhang, N.; Hong, Y.; Yazdanparast, S.; et al. Superior structural, elastic and electronic properties of 2D titanium nitride MXenes over carbide MXenes: A comprehensive first principles study. *2d Mater.* **2018**, *5*, 045004.
44. Mego, K.; Accardo, E.; Ruiz-Campos, P.; et al. $CsPbBr_3$ nanocrystals supported on a partially oxidized Ti_2N MXene for photothermal CO_2 conversion. *Mater. Adv.* **2026**, *7*, 2465–2480.
45. Cai, Y.S.; Chen, J.Q.; Su, P.; et al. Atomically precise metal nanoclusters combine with MXene towards solar CO_2 conversion. *Chem. Sci.* **2024**, *15*, 13495–13505.
46. Zhang, L.; Zhang, J.; Yu, J.; et al. Charge-transfer dynamics in S-scheme photocatalyst. *Nat. Rev. Chem.* **2025**, *9*, 328–342.
47. Su, T.; Hood, Z.D.; Naguib, M.; et al. 2D/2D heterojunction of Ti_3C_2/gC_3N_4 nanosheets for enhanced photocatalytic hydrogen evolution. *Nanoscale* **2019**, *11*, 8138–8149.
48. Cabrero-Antonino, M.; Uscategui-Linares, A.; Ramírez-Grau, R.; et al. 2D/2D MOF/MXene schottky junction: Prolonged carrier lifetime and enhanced hydrogen evolution efficiency. *Angew. Chem. Int. Ed.* **2025**, *64*, e202503860.
49. Qiang, W.; Qu, X.; Chen, C.; et al. Ti_3C_2 MXene derived (001) TiO_2/Ti_3C_2 heterojunctions for enhanced visible-light photocatalytic degradation of tetracycline. *Mater. Today Commun.* **2022**, *33*, 104216.
50. Low, J.; Zhang, L.; Tong, T.; et al. TiO_2/MXene Ti_3C_2 composite with excellent photocatalytic CO_2 reduction activity. *J. Catal.* **2018**, *361*, 255–266.
51. He, F.; Zhu, B.; Cheng, B.; et al. 2D/2D/0D $TiO_2/C_3N_4/Ti_3C_2$ MXene composite S-scheme photocatalyst with enhanced CO_2 reduction activity. *Appl. Catal. B Environ.* **2020**, *272*, 119006.
52. Quyen, V.T.; Ha, L.T.T.; Thanh, D.M.; et al. Advanced synthesis of MXene-derived nanoflower-shaped TiO_2@Ti_3C_2 heterojunction to enhance photocatalytic degradation of Rhodamine B. *Environ. Technol. Innov.* **2021**, *21*, 101286.
53. Hieu, V.Q.; Lam, T.C.; Khan, A.; et al. TiO_2/Ti_3C_2/g-C_3N_4 ternary heterojunction for photocatalytic hydrogen evolution. *Chemosphere* **2021**, *285*, 131429.
54. Xu, F.; Mei, W.; Hu, P.; et al. Spatially Engineered Ternary Schottky/S-Scheme Heterojunctions for Artificial Photosynthesis. *Angew. Chem. Int. Ed.* **2025**, *64*, e202513364.
55. Mei, W.; Zhao, F.; Xu, K.; et al. Schottky−Defect–Photothermal Coupling in Nb_2C/Nb_2O_{5-x} Heterostructures for Enhanced CO_2 Photoreduction. *ACS Catal.* **2026**, *16*, 5115–5127.
56. Liu, H.; Shi, L.; Zhang, Q.; et al. Photothermal catalysts for hydrogenation reactions. *Chem. Commun.* **2021**, *57*, 1279–1294.
57. Anouar, A.; Dhakshinamoorthy, A.; Xu, F.; et al. Engineering MXenes for Thermal and Photothermal Catalysis. *Chem. Rev.* **2026**, *126*, 3664–3729.
58. Li, R.; Zhang, L.; Shi, L.; et al. MXene Ti_3C_2: An effective 2D light-to-heat conversion material. *ACS Nano* **2017**, *11*, 3752–3759.
59. Guzelturk, B.; Kamysbayev, V.; Wang, D.; et al. Understanding and controlling photothermal responses in MXenes. *Nano Lett.* **2023**, *23*, 2677–2686.

60. Tian, L.; Xu, F.; Sastre, G.; et al. Engineering MXene surfaces and heterostructure interfaces for efficient heterogeneous catalysis. *Chem. Soc. Rev.* **2026**, *55*, 4244–4302. https://doi.org/10.1039/D5CS00376H.
61. Kruger, D.D.; Cabrero-Antonino, M.; Osella, S.; et al. Surface-State–Regulated Product Distribution in Photothermal CO_2 Hydrogenation over MXene-Based S-Scheme Catalyst. *Angew. Chem. Int. Ed.* **2026**, e8425918.